Emerging Microbes & Infections
2025, VOL. 14, 2552783 (19 pages)
https://doi.org/10.1080/22221751.2025.2552783

Conserved multiepitopes in *Plasmodium falciparum* STEVORs enable rational design of a fusion antigen vaccine construct with broad immunogenicity

Zhi-Shan Sun[a,b,c,d,e*], Jing-Xian Yin[a], Han-Qing Zhao[a], Yin-shan Zhu[a], Shen-Bo Chen[b,c,d,e], Hai-Mo Shen[b,c,d,e], Bin- Xu[b,c,d,e], Xiao-Nong Zhou[a], Tian-Yu Wang[b,c,d,e], Wan-Xuan Yang[f], Yi-Wen Duan[b,c,d,e], Jun-Hu Chen[b,c,d,e,f] and Kokouvi Kassegne [a]

[a]School of Global Health, Chinese Centre for Tropical Diseases Research, Shanghai Jiao Tong University School of Medicine, Shanghai, People's Republic of China; [b]National Key Laboratory of Intelligent Tracking and Forecasting for Infectious Diseases, National Institute of Parasitic Diseases, Chinese Center for Disease Control and Prevention (Chinese Center for Tropical Diseases Research), Shanghai, People's Republic of China; [c]National Health Commission of the People's Republic of China (NHC) Key Laboratory of Parasite and Vector Biology, Shanghai, People's Republic of China; [d]World Health Organization (WHO) Collaborating Center for Tropical Diseases, Shanghai, People's Republic of China; [e]National Center for International Research on Tropical Diseases, Shanghai, People's Republic of China; [f]Hainan Tropical Diseases Research Center (Hainan Sub-Center, Chinese Center for Tropical Diseases Research), Haikou, People's Republic of China

ABSTRACT

There is no vaccine for severe malaria. STEVOR antigens on the surface of *Plasmodium falciparum*-infected red blood cells are implicated in severe malaria and are targeted by neutralizing antibodies, but their epitopes remain unknown. Using computational immunology, we identified highly immunogenic overlapping B- and T-cell epitopes (referred to as multiepitopes, 7–27 amino acids) in the semiconserved domain of four STEVORs linked with severe malaria and clinical immunity. Structural analyses confirmed the conservation in homologous sequences across 138 clinical isolates (Togo and Brazil) and 342 global strains. Designed fused multiepitopes showed high IgG antibody reactivity in the sera of *P. falciparum*-infected individuals. The fused multiepitopes had no allergenicity/toxicity, and phenotyping via flow cytometry and immunological assays revealed the induction of CD4+ and CD8+ T-cell proliferation and IgG antibodies in BALB/c mice, respectively. On this basis, structure-guided design of a multiepitope fusion antigen (MEFA) vaccine construct achieved 97.15% global combined HLA coverage and elicited both cellular and humoral immunity *in silico*. Recombinant MEFA was stably expressed in *Escherichia coli* and recognized significantly more anti-STEVOR IgG antibodies in the sera of nonsevere malaria cases than in those of severe cases, underscoring its potential immunogenicity and association with milder disease. The STEVOR MEFA construct emerges as a promising severe malaria vaccine candidate, combining global HLA coverage, safety, and broad immunogenicity linked to milder clinical outcomes.

Abbreviations: VSAs: Variant surface antigens; STEVORs: Subtelomeric variable open reading frames; iRBCs: Infected red blood cells; RBCs: Red blood cells; *rifs*: Repetitive interspersed families; SP: Signal peptide; V1: First variable; V2: Second variable; PEXEL: *Plasmodium* export element; SC: Semiconserved; TM1: First transmembrane; TM2: Second transmembrane; C: C-terminus; GPC: Glycophorin C; WHO: World Health Organization; IEDB: Immune Epitope Database; MHC-I: Major histocompatibility complex class I; NCBI: National Center for Biotechnology Information; HLA: Human leukocyte antigen; PCR: Polymerase chain reaction; GRAVY: Grand average of hydropathicity; IgM: Immunoglobulin M; IgG: Immunoglobulin G; APCs: Antigen-presenting cells

ARTICLE HISTORY Received 17 March 2025; Revised 15 August 2025; Accepted 22 August 2025

KEYWORDS *Plasmodium falciparum*; severe malaria; STEVOR; multiepitope; immunogenicity; vaccine construct

Introduction

Malaria is an infectious disease caused by *Anopheles* mosquito bites, which transmit *Plasmodium* parasites into humans. In 2023, approximately 263 million malaria cases and 597,000 malaria-related deaths were reported across 83 malaria-endemic countries worldwide [1]. Among the five species of *Plasmodium* that regularly infect humans, *Plasmodium falciparum* causes severe malaria [2], which occurs mainly in children and pregnant women and results in at least 400,000 deaths per year [3]. Variant surface antigens (VSAs) are major families of antigen genes expressed on the surface of *P. falciparum*-infected red blood cells (iRBCs). Notably, *var* genes, n ≈ 60; repetitive

CONTACT Jun-Hu Chen chenjh@nipd.chinacdc.cn National Key Laboratory of Intelligent Tracking and Forecasting for Infectious Diseases, National Institute of Parasitic Diseases, Chinese Center for Disease Control and Prevention (Chinese Center for Tropical Diseases Research), Shanghai, People's Republic of China; Kokouvi Kassegne ephremk@hotmail.fr School of Global Health, Chinese Centre for Tropical Diseases Research, Shanghai Jiao Tong University School of Medicine, Shanghai 200025, People's Republic of China
*Present Address: Haining Center for Disease Control and Prevention, Haining, Zhejiang 314400, People's Republic of China
Supplemental data for this article can be accessed online at https://doi.org/10.1080/22221751.2025.2552783.

interspersed families (*rifs*), n ≈ 159; and subtelomeric variant open reading frames (*stevors*), n ≈ 30 [4,5], play roles in the development of severe malaria [6–8]. Severe malaria, a lethal complication of *P. falciparum* infection, arises from parasite sequestration in vital organs via cytoadherence of iRBCs to vascular endothelium and rosette formation. These processes trigger microcirculatory obstruction, systemic inflammation, and tissue hypoxia, culminating in life-threatening manifestations like cerebral malaria, severe anaemia, and metabolic acidosis. Rosetting is a key determinant of severe malaria and refers to clustering uninfected RBCs bound to a central iRBC, forming a flower-like structure [9], which can obstruct microvascular blood flow [10]. STEVORs are involved in rosetting and altering RBC deformability by binding with glycophorin C (GPC) on RBCs [7,11].

STEVORs colocalize with *P. falciparum* merozoite surface protein 1 (MSP1) MSP1 on invading merozoites, and their functional necessity in the invasion machinery essential for parasite survival is demonstrated by anti-STEVOR antibodies (antiS1/antiS2), which block erythrocyte adhesion in a variant-specific manner [7]. Additionally, STEVORs drive P. falciparum erythrocyte membrane protein 1 (PfEMP1)-independent rosetting through GPC binding. Elevated STEVOR expression in rosetting-positive clones and 50% rosette inhibition by anti-STEVOR antibodies pinpoints STEVOR – GPC interactions and confirms their role [7]. STEVORs consist of a signal peptide (SP), a first variable (V1) domain, a *Plasmodium* export element (PEXEL) motif, a semiconserved (SC) domain, a first transmembrane (TM1) domain, a second variable (V2) domain, a second transmembrane (TM2) domain, and a conserved C-terminus (C) [12], with the SC region exposed on the surface of iRBCs [13]. The SC region of STEVOR is driven by point mutations and localized indels, yet not all variants are functionally equivalent [7,14]. From over 30 STEVORs in *P. falciparum* 3D7, we prioritized four candidates based on their established roles in pathogenesis and immunogenicity: (i) PF3D7_1040200 and PF3D7_0617600 were selected because they mediate PfEMP1-independent RBC adhesion – rosetting via GPC receptor binding, and their SC regions are targets of antibodies that inhibit both merozoite invasion and rosette formation – key virulence mechanisms [7]; (ii) PF3D7_0115400 and PF3D7_0300400 were included due to their association with cerebral malaria susceptibility in clinical studies [15], and their immunodominant SC regions, which elicit high serum reactivity in peptide microarrays [12]. This targeted approach ensures that our multiepitope fusion antigen focuses on STEVOR variants with empirically validated roles in severe disease and clinical immunity, maximizing translational potential.

There is currently no vaccine that provides complete protection against severe malaria. However, VAR2CSA, a specific VSA of the PfEMP1 which binds with chondroitin sulphate A in the placenta [16], is currently a vaccine candidate antigen against placental malaria, with two vaccine candidates (PAMVAC and PRIMVAC) currently in phase Ia/Ib clinical trials [17]. This suggests the potential of VSAs for vaccine candidates and antigen candidates can also be found in STEVORs.

Although STEVORs are involved in rosetting and are recognized by the host immune system, the immune characteristics associated with the functional immunogen regions in the SC region of STEVORs are unknown. A significant obstacle in developing VSAs, including STEVORs, as vaccine candidates is their antigenic diversity [18], and the approach of conserved epitopes is an alternative to overcome antigen diversity.

In this study, we focused on the structural and functional domains of STEVORs and applied computational immunology to select relatively conserved, highly immunogenic, nontoxic, nonallergenic, hydrophilic T- and B-cell epitopes (referred to as multiepitopes) from the SC domain of STEVORs. These STEVORs include PF3D7_1040200, PF3D7_0617600, PF3D7_0115400 and PF3D7_0300400 (hereafter referred to as ST1, ST2, ST3, and ST4, respectively). Multiepitopes from the selection were assessed for conservation via homologous sequences of clinical isolates/global strains and were thereafter combined to obtain multiepitope fusion epitopes. To assess the antigenicity and safe immunogenicity of the fused multiepitopes, we explored anti-STEVOR immunoglobulin G (IgG) antibodies in the sera of subjects naturally exposed to *P. falciparum* infections and in immunized mice. Additionally, we assessed the correlation between amino acid conservation within and the antibody response to the multiepitopes. Finally, we designed a multiepitope fusion antigen (MEFA) vaccine construct and assessed immunonogenicity via *in silico* tests.

Materials and methods

The overall design and methodology of this study are summarized in Figure S1.

Ethical considerations

The malaria samples were collected under approval (N °019/2019/MSHP/CBRS) from the Togolese Ministry of Health's Bioethics Committee [19,20]. Normal control group (NCG) samples were collected in Shanghai, China, with the approval (No. CMEC-2021-KT-15) of the Ethics Committee of the Shanghai Jiao Tong University School of Medicine Xinhua Hospital, Chongming Branch. Written informed consent was obtained from all participants prior to sample collection. All

the data were anonymized and handled confidentially in strict accordance with the Declaration of Helsinki. All animal handling and experimental procedures were conducted in accordance with ethical guidelines, and the Ethics Committee of Hainan Tropical Diseases Research Center approved the study under Grant No. WSJK2024MS226.

Sequence retrieval and mapping of the structural domain

The sequences of all 32 STEVORs of *P. falciparum* 3D7, including those of ST1, ST2, ST3 and ST4, were retrieved from PlasmoDB (https://plasmodb.org/plasmo, accessed on May 23, 2024) and imported into Jalview software (https://www.jalview.org/) for alignment. To obtain more accurate protein domains, SignalP-6.0 (https://services.healthtech.dtu.dk/services/SignalP-6.0/) and Deep TMHMM (https://dtu.biolib.com/DeepTMHMM) were utilized to identify the SP and TM domains of the protein, respectively. On the basis of previous studies [12,18], the domains of the four STEVORs were finally sorted.

Identification of B-cell epitopes and T-cell epitopes

Linear B-cell epitopes from the full-length sequences of the four STEVORs were predicted via the Immune Epitope Database (IEDB) B-cell epitope prediction tools (http://tools.iedb.org/main/bcell/). B-cell epitopes within the SC domain were predicted using BepiPred-2.0 (IEDB) with a stringent threshold (> 0.55), corresponding to 81.7% specificity and 29.2% sensitivity per the IEDB benchmarks. This cut-off prioritized high-confidence epitopes to minimize false positives, a critical consideration for vaccine design. Consistent with reported B-cell epitope characteristics – typically spanning 5–17 amino acids – we set a minimum length of five residues to ensure biological relevance while accommodating structural variability [21]. Discontinuous epitopes are residues that are not sequential in the primary structure of protein but are brought together in the 3D structure [22]. The 3D structure models of the four STEVORs were submitted to ElliPro (http://tools.iedb.org/ellipro/) to validate the discontinuous epitopes.

CD8+ T-cell epitopes were predicted using the IEDB Next-Generation Tools pipeline (https://nextgen-tools.iedb.org/pipeline), with a percentile rank cut-off value < 0.5 (corresponding to 85% sensitivity and 90% specificity per IEDB validation data) [23]. CD4+ T-cell epitopes were identified via IEDB MHC-II binding simulations (http://tools.iedb.org/mhcii/), with a percentile rank < 2 (80% sensitivity and 85% specificity for MHC-II binders) [23]. These stringent thresholds ensure the selection of strong major histocompatibility complex binders – high-affinity epitopes – critical for vaccine-induced immunity. The full human leukocyte antigen (HLA) reference set was selected for T-cell epitope identification.

Analysis of the physicochemical properties of the epitopes

B-cell epitopes overlapping with CD8 + and CD4+ T-cell epitopes were initially selected and referred to as multiepitopes. The low-complexity region was analysed via PlasmoDB. The hydrophilicity, surface accessibility, and antigenicity statuses of the epitopes were assessed via the DNAStar Protean system (DNASTAR, Inc., Madison, Wisconsin, USA) and Vaxijen (https://ddg-pharmfac.net/vaxijen/VaxiJen/VaxiJen.html). Allergenicity and toxicity were predicted via AllerTop v.2.0 (https://ddg-pharmfac.net/AllerTOP/) and ToxinPred2 (https://webs.iiitd.edu.in/raghava/toxinpred2/index.html), respectively.

Conservation analysis

To identify similarities between the STEVORs and human proteins, as well as the potential risk of autoimmune responses, sequences of the four STEVORs were imported into PlasmoDB (https://plasmodb.org/plasmo) and the National Center for Biotechnology Information (NCBI, https://ncbi.nlm.nih.gov/) for BLASTP. STEVOR protein sequences were compiled from 133 clinical isolates from Togo (3D7 strain) sourced from this study, and 5 clinical isolates from Brazil (7G8 strain) and 342 nonclinical sequences representing 22 global strains (including 3D7 = 33, 7G8 = 8, Dd2 = 11, HB3 = 16, and NF54 = 19) sourced via BLASTP from NCBI and PlasmoDB. This comprehensive dataset captured both geographic diversity (Togo, Brazil) and strain variation for robust conservation analysis (Tables S1–4). The DNA of *P. falciparum* clinical isolates from Togo [19, 20] was used for polymerase chain reaction (PCR) amplification of the *stevor* genes with the primers and reaction conditions provided in Tables A1–2. The PCR products were confirmed by 2% agarose gel electrophoresis, visualized under a Tanon MINI space 2000 (Tanon, Shanghai, China), and sent to the BGI Group (Shanghai, China) for sequencing.

All the sequence reads were imported into MegAlign software (DNAStar, WI, America) and aligned via the ClustalW method, and the sequences of the target genes were intercepted. The aligned sequences were submitted to Weblogo (https://weblogo.berkeley.edu/logo.cgi) to visualize amino acid (AA) conservation. Additionally, AA entropy was calculated from sequence alignment via Shannon Entropy-One (https://www.hiv.lanl.gov/content/sequence/ENTROPY/entropy.html). The average AA mutation rates for each reference multiepitope were calculated,

as were the differences in AA mutation rates among different sample sources via the Kruskal–Wallis test.

Preparation of multiepitopes and serum samples

Plasmodium falciparum merozoite surface protein 1 (MSP1) is a leading vaccine candidate against infection [24]. We selected B-cell and T-cell epitopes (^{384}FTDPLELE^{391} and ^{217}QIPFNLKIRANELDVLKKLV^{236}, respectively) from *P. falciparum* MSP1 block p83 to generate a multiepitope as a positive control. Fused multiepitopes were constructed by concatenating all predicted multiepitopes from each STEVOR variant (ST1, ST2, ST3, and ST4) without linker sequences to preserve native antigenicity. The most immunogenic, nontoxic, and nonallergenic fusion per variant was prioritized for synthesis. For ST2, which yielded only one qualifying multiepitope, this candidate was advanced directly to production. The four fused multiepitope sequences (referred to as ST1-Grp, ST2-Grp, ST3-Grp, and ST4-Grp) and the positive control multiepitope sequence (referred to as MSP1$_{_p83}$) were chemically synthesized by Shanghai Qiangyao Biological (Shanghai, China) via the Fmoc synthesis method at 95% purity in the form of lyophilized powder, with 9-fluorenylmethoxycarbonyl added to the C-amino end to protect epitope activity. The multiepitopes were homogenized to 1 mg/ml and diluted to 2 μg/ml in phosphate-buffered saline (PBS) for further use.

Human blood samples were collected from a cross-sectional malaria surveillance study (April–November 2019) in two endemic regions of Togo: Agou-Gadzépé (7°28'N; 1°55'E; population ~11,000) and Atakpamé (7°53'N; 1°13'E; population ~84,979). These sites experience tropical climate with biannual rainy seasons (April–October) that drive malaria transmission peaks. The articipants were screened by microscopy for *P. falciparum* infection, with PCR confirmation [19,20]. The study population demographics, including age distribution, clinical malaria status, and parasite densities are presented in Table A3. Serum samples were discarded and stored as dried spots on 903 protein-saving cards (Whatman, UK). Malaria cases < 14 years old were prioritized for this study and were divided into severe malaria (SMG, n = 61) and uncomplicated or nonsevere malaria (NMG, n = 72) groups according to parasite density and clinical manifestations, following the WHO criteria for severe malaria and other studies [25–27]. Malaria cases with both a parasite density >100,000/μL and at least one clinical marker of severity (prostration, jaundice, vomiting, severe breathlessness, dark urine, or multiple convulsions) were classified into the SMG group [27], whereas the NMG group include uncomplicated cases (parasite density <100,000/μL without severe symptoms).

The normal control (NCG) cohort was carefully designed to account for both: (1) Togolese uninfected individuals (n = 21; age 13–32 years; PCR-confirmed negative, and ≥6 weeks without malaria exposure) to account for potential prior immunity; and (2) Chinese nonendemic controls (n = 20; age 30–43 years; PCR negative, and no malaria history) to establish antibody-naive baselines [20]. The Togo endemic cohort controls for background exposure (ruling out cross-reactivity), while the China cohort provides a true negative baseline. This dual-design strengthens specificity claims and ensures transparency in interpreting baseline immune responses. All were asymptomatic at sampling (Table A3).

In vivo *immunogenicity assessment via immunization of BALB/c mice*

Female BALB/c (6-week-old) mice were purchased from Shanghai Jihui Laboratory Animal Breeding (Shanghai, China) and were housed in an SPF-class mouse husbandry room under a controlled environment of regulated temperature, ventilation and ambient humidity.

The immunization protocol was performed as previously described [28–30], with minor modifications. Briefly, 42 mice were divided into seven groups (n = 6 per group) comprising one adjuvant control (Freund's Adjuvant, Sigma–Aldrich, USA) group; four experimental groups, namely, the ST1-Grp, ST2-Grp, ST3-Grp, and ST4-Grp-fused multiepitopes formulated in the adjuvant; one PBS control group (PBS formulated in the adjuvant), and one MSP1$_{_p83}$ positive control group. Blood samples (100–50 μL per draw) were collected from mouse tail veins at five time points: 0 (baseline), 14, 28, 42, and 56 days postimmunization. Body weights were recorded before and after each collection to monitor health status. Following the final blood collection on day 56, the mice were humanely euthanized by cervical dislocation (Figure 3A). Groups received subcutaneous injections (100 μL) as follows: (1) adjuvant control (PBS emulsified in adjuvant), (2) PBS control (PBS alone), (3) experimental groups (ST1-Grp, ST2-Grp, ST3-Grp, or ST4-Grp at 0.5 mg/mL emulsified in adjuvant), and (4) positive control (MSP1$_{_p83}$ at 0.5 mg/mL emulsified in adjuvant). Immunizations were administered on days 1 (prime), 15, 29, and 43 (boosts) following standard protocols as described above. The adjuvant emulsion was prepared under sterile conditions by homogenizing the aqueous antigen solution (ST1-Grp, ST2-Grp, ST3-Grp, ST4-Grp, PBS, or MSP1$_{_p83}$) with the oil phase at a 1:1 v/v ratio via high-speed vortexing to ensure molecular integrity and immunogenicity. Except for the PBS control group, the other groups received Freund's complete adjuvant during the first injection and Freund's incomplete adjuvant during subsequent injections. At each

blood collection, the samples were allowed to coagulate at room temperature (RT) for one hour, after which the serum was transferred into 1.5 ml EP tubes and stored at -20°C.

Detection of IgG antibodies

For total IgG level assays, 100 µl of 2 µg/ml fused multiepitope mixture in coating buffer (Sangon Biotech, China) (1:100 dilution of 200 µg/ml multiepitope mixture in 1× coating buffer) was coated into a 96-well Coat Nunc ™ F96 MicroWell ™ plate (Thermo Fisher Scientific, USA) in duplicate and incubated overnight at 4°C. The plates were then washed three times with 200 µl/well of 1×PBS with Tween 20 (PBST) wash buffer, blocked with 200 µl/well of 1×ELISA Diluent (Invitrogen, USA) and incubated at RT for two hours. One hundred microliters of serum from malaria patients (1:500 in 1×ELISA Dilluent) or 1×ELISA Diluent (negative serum control) was added to each well and incubated at RT for two hours. The plates were washed as described above, and 100 µl/well (1:10,000) of goat anti-human IgG Fc horseradish peroxidase (HRP) preabsorbed (Abcam, UK) was added for incubation at RT for one hour. The plates were washed, and 100 µl of 1× TMB (3,3′,5,5’-tetramethylbenzidine) solution (APExBIO, USA) was added to each well and then incubated at RT for 10 min for antibody detection. The IgG antibodies were visualized by adding 100 µl/well of ELISA Stopping Solution (Sangon Biotech, China) and then quantified at 450 nm via a BioTek Synergy HTX Multimode Reader (Agilent Technologies, USA). The assays were also performed with serum samples from the uninfected and unexposed NCG groups from China, and Togo.

Total IgG antibody responses in serum samples from immunized mice were also assessed by ELISA as described above. HRP-conjugated goat anti-mouse IgG Fc-specific antibody (Sigma–Aldrich, USA) at a 1:40,000 dilution was used for antibody detection. While quadruplicates may be standard in murine studies (where sample volume permits), our use of duplicates was a deliberate and statistically justified by cross-study harmonization. Maintaining duplicates for both human and mouse ELISAs ensured direct comparability of immunogenicity data – a critical factor given our translational framework linking preclinical and clinical results.

Detection of interferon-gamma (IFN-γ) and interleukin-2 (IL-2)

The levels of IFN-γ and IL-2 in serum of the immunized mice reflect broader immunogenicity. These circulating cytokines were quantified via commercial ELISA kits (Mouse lFN gamma Uncoated ELISA Kit [Thermo Fisher Scientific, USA] and Mouse IL-2 Uncoated ELISA Kit [Thermo Fisher Scientific, USA]) following the manufacturers’ instructions. The concentration of each cytokine was determined via interpolation in a curve set with the standards supplied by the kit.

Flow cytometry

To assess the proliferation of total CD8+ T cells and CD4+ T cells in mouse splenocytes, T-cell phenotyping (without antigen stimulation) via flow cytometry was performed by Dakewe Biotech (Shenzhen, China). Under sterile conditions, the mice were dissected, the spleens were isolated, and single-cell suspensions were prepared as follows. Spleens were cut into several pieces in precooled sterile PBS and then ground in a 70 µm filter with a syringe piston. The filter was rinsed with 15 ml of PBS, after which it was collected and centrifuged at 350 × g for five minutes, after which the supernatant was discarded. Thereafter, 3 ml of 1× RBC lysis buffer (10× RBC Lysis Buffer, BioLegend, USA) was added, and the cells were resuspended and incubated on ice for five minutes. Lysis of RBCs was stopped by adding 10 ml of PBS, followed by centrifugation at 350 × g for five minutes, and the supernatant was discarded. The steps were repeated to ensure efficient cell lysis.

The cell concentration was adjusted to 1×10^7/ml to count live cells, and 100 µl was taken from each sample to prepare 1×10^6 cells/tube. A single fluorescently labelled antibody (APC anti-mouse CD4 antibody, Cat. 100516; PE/Cyanine7 anti-mouse CD8a antibody, Cat. 100722) was used to stain specific cell surface antigens, followed by incubation for 20 min in the dark. Two millilitres of PBS were added to resuspend the cells, followed by centrifugation at 350 × g for five minutes. The supernatant was subsequently discarded, and 300 µl of PBS was added to resuspend the cells. Flow cytometry was performed via CytoFLEX S (Beckman Coulter, Brea, USA), and the data were analysed via CytExpert software.

Design and physicochemical properties of a multiepitope fusion antigen vaccine construct

To facilitate future vaccine candidate selection and optimization, we designed a multiepitope fusion (MEFA) vaccine construct that included the fused multiepitopes of the four STEVORs. Adjuvants can increase antigenicity and increase the efficiency of vaccines [31], and beta-defensins have been widely explored as potential adjuvants to increase the immunogenicity and efficacy of multiepitope vaccines [32]. Therefore, we added beta-defension-3 (UniProtKB: Q5U7J2) as an adjuvant to enhance the immunogenicity of the MEFA vaccine construct. Additionally, the “EAAAK” linker was included to connect the adjuvant to CD8+ T-cell epitopes, whereas the AAY, GPGPG, and KK linkers were used to link CD8

+ T cells, CD4+ T cells, and B-cell epitopes, respectively. Overall, the vaccine construct was designed such that the epitopes are listed in ascending order of antigenicity. When a vaccine is injected, its main duty is to trigger an immune response in host cells. Therefore, VaxiJen v2.0 (https://www.ddg-pharmfac.net/vaxijen/VaxiJen/VaxiJen.html) was used to predict the antigenicity of the vaccine construct. In addition, the grand average of hydropathicity (GRAVY), aliphatic index, instability index, and estimated half-life in mammals, yeast, and *Escherichia coli* were predicted via ProtParam (https://web.expasy.org/protparam/). AllerTop v2.0 (https://www.ddg-pharmfac.net/AllerTOP/) and ToxinPred 2 (https://webs.iiitd.edu.in/raghava/toxinpred2/) were used to predict allergenicity, and toxicity was assessed as described above.

Population coverage and structure of the MEFA vaccine construct

A total of nine CD4+ T-cell epitopes and eleven CD8+ T-cell epitopes of the vaccine construct, as well as the corresponding HLA-I and HLA-II alleles, were submitted to the IEDB population coverage website (http://tools.iedb.org/population/) to calculate the proportion of individuals predicted to respond to the epitope set on the basis of the alleles.

The secondary structure of the multiepitope vaccine construct was predicted via the prabi (https://npsa-prabi.ibcp.fr/cgi-bin/npsa_automat.pl?page=/NPSA/npsa_gor4.html) server. The three-dimensional (3D) structure of the vaccine construct was predicted via Alphafold3 (https://alphafoldserver.com/) [33]. Additionally, a Ramachandran plot was generated with PROCHECK (https://saves.mbi.ucla.edu/) to verify the integrity and quality of the structure.

Immune simulation analyses

The full sequence of the vaccine candidate was subjected to C-IMMSIM (https://kraken.iac.rm.cnr.it/C-IMMSIM/index.php) to characterize immune responses. The HLA selection parameters for MHC-I were set to HLA-A*03:01, HLA-A*68:02, HLA-B*08:01, and HLA-B*15:01; the parameters for DR MHC-II were set to HLA-DRB4*01:01 and HLA-DRB3*01:01. Three injections of 1000 vaccine particles were given at four-week intervals with the time step of injection set to 1, 84, and 168 (each time step was 8 h, and time step 1 was injection at time = 0). The total number of simulation steps was set to 1050.

Molecular docking of the MEFA vaccine construct

To validate the immunogenic potential of our MEFA vaccine construct, we performed molecular docking between the MEFA-HLA-DRB1*04:01 complex (PDB ID: 5NI9) and a crystallographically resolved T-cell receptor (TCR; PDB ID: 3T0E) via the ZDOCK server (https://zdock.wenglab.org/). This approach is critical because HLA-DRB1*04 alleles are genetically associated with severe *P. falciparum* malaria [34], and TCR recognition of peptide – MHC complexes is essential for T-cell activation – a cornerstone of adaptive immunity [35]. By simulating this interaction, we ensured structural compatibility between the MEFA-presented epitopes and the complementarity-determining regions (CDRs) of TCR, thereby confirming mechanistic plausibility and predicting robust immune responses. This docking strategy aligns with recent advances in epitope-based vaccine design, emphasizing the need for *in silico* validation to avoid misfolding or steric clashes that could compromise immunogenicity. The use of a prevalidated TCR-HLA-DRB1*04:01 structure provided a biologically relevant framework to assess binding stability and epitope accessibility, ensuring our MEFA construct meets the energetic and spatial requirements for effective T-cell priming.

Recombinant expression, purification, and validation of the MEFA construct

The MEFA and $MSP1_{-42}$ (positive control) genes were codon-optimized for *Escherichia coli* expression (GenScript, China) and cloned into pET-30a with C-terminal 6×His tags (Figure S2). Following transformation into BL21(DE3) via heat shock, the proteins were expressed in Luria–Bertani (LB) medium (37°C, 200 rpm), with expression confirmed by SDS-PAGE. For large-scale production, cultures were expanded in Terrific Broth, induced with β-D-1-thiogalactopyranoside (IPTG) (15°C, 16 h), and harvested by centrifugation. Cell lysates, prepared via sonication, underwent Ni-affinity chromatography, followed by sterilization (0.22 μm filtration) and quantification (Bradford assay, with BSA as a standard). Purity and molecular weight were verified by SDS-PAGE (4–20% gradient gel for electrophoretic separation; GenScript, China) under reducing/nonreducing conditions (300 mM Tris-HCl/250 mM DTT [pH 6.8] and 250 mM Tris-HCl/400 mM DTT [pH 6.5], respectively) and Western blot, to ensure structural integrity for downstream validations.

The immunogenic potential of the purified MEFA protein was validated *ex vivo* via ELISA by quantifying total IgG antibody levels in serum samples from *P. falciparum*-infected Togo subjects (SMG, n = 61 and NMG, n = 72 groups) and NCG groups (Togolese endemic controls (n = 21) and Chinese nonendemic controls (n = 20), with recombinant $MSP1_{-42}$ serving as the positive control). The ELISA protocol followed standardized methods as detailed in earlier sections, ensuring consistency across assays. This approach aimed to confirm

antigen-specific humoral responses while establishing baseline reactivity across clinical and control cohorts and to ensure the capacity of MEFA construct to elicit biologically relevant antibody responses.

Statistical analyses

All human and mouse serum samples were tested in duplicate wells to ensure assay consistency and reproducibility, with experimental data calculated as the mean OD of duplicates minus the negative control (PBS) mean. To establish a stringent seropositivity threshold, we defined the cut-off value as the mean OD of our combined NCG groups (PCR-negative Togolese individuals with ≥6 weeks malaria-free status and malaria-naive Chinese controls) plus 2 standard deviations (2SD). This statistically robust threshold – widely adopted in immunological studies including WHO malaria serology guidelines – optimally balances sensitivity (detecting true positives) and specificity (minimizing background reactivity), while remaining clinically relevant for detecting partial immunity in endemic populations. Samples exceeding this validated threshold were classified as seropositive.

The chi-square test was used when two rates were compared. The Kruskal–Wallis test was used to test whether there were differences between groups. Furthermore, multiple comparisons between groups were performed via the command "pairwise_wilcox_test" in the R package "rstatix." All the data were analysed and visualized with R 4.4.2 (R Foundation for Statistical Computing, Austria) with R Studio (Posit, USA) and GraphPad Prism 9. We also performed Spearman correlation analyses between multiepitope conservation/variability and the antibody level (OD at 450 nm) and the percentage of positive serum samples. For all analyses, a P value (*$P < 0.05$, ** $P < 0.01$, *** $P < 0.001$) was considered statistically significant.

Results

Structural architecture of STEVOR proteins reveals conserved functional domains

Comprehensive structural analysis of all 32 STEVOR proteins in *P. falciparum* 3D7 confirmed a conserved domain architecture comprising the SP, variable (V1/V2), PEXEL, SC, TM1/TM2, and C-terminal domains (Figure S3). Notably, our focused investigation of ST1 – ST4 revealed that their SC domains – spanning residues [53–182 AA] (Table A4) – maintained critical structural integrity. This precise domain mapping enabled strategic selection of the SC region as our target for multiepitope identification, balancing conservation for broad coverage with variability for immune recognition.

STEVORs harbour immunogenic B- and T-cell multiepitopes in their semiconserved domains

Our systematic analysis identified nine high-potential multiepitopes within the semi-conserved (SC) domains of four STEVOR antigens, as follows: ST1: ^{54}QNHNPHYHND^{63} (10 AA), ^{89}KQLKEVVEKNGT KIRGGNSAE^{109} (21 AA), and ^{123}EDVFGDKN-HAMLKSGRYPNDDDESDDS^{149} (27 AA); ST2: ^{100}TKPVGEHGTEP^{110} (11 AA); ST3: ^{78}IKKYQNT^{84} (7 AA) and ^{100}TKHVGGNDTEP^{110} (11 AA); and ST4: ^{78}IKKYQQT^{84} (11 AA), ^{96}EKNGTKYSGGN-DAEP^{110} (20 AA), and ^{123}EEIFGNESDMLKSG MSPNVD^{142}. Each multiepitope demonstrated: (1) dual recognition capability through overlapping T-cell (both MHC I/II-restricted) and B-cell (linear/conformational) epitope sites (Figure 1(A–D), Tables S5-S6); (2) optimal vaccine characteristics with strong predicted antigenicity (VaxiJen >0.66), nontoxicity, and nonallergenicity; and (3) broad population coverage through binding to diverse HLA alleles (Table S7). These findings position the SC domain as a strategic target for a STEVOR multiepitope vaccine.

Conservation analysis reveals stable multiepitopes targets across geographic strains

Our comprehensive conservation analysis demonstrated strong preservation of the selected multiepitopes, with agarose gel electrophoresis confirming successful epitope amplification across all the targets (Figure S4). Notably, Togo clinical isolates exhibited exceptional sequence conservation, with ST2–ST4 epitopes showing significantly greater AA identity in local strains (Tables S8–S11) than in global variants (Table 1, Tables S12–S19). This geographic conservation pattern was particularly pronounced for the ST4 epitopes, which presented the lowest AA entropy values (Figure 1(E)), suggesting structural or functional constraints. While the ST1 epitopes showed greater variability, the overall high conservation (mean AA identity >85%) across all the targets validates their suitability as vaccine candidates.

Multiepitope-specific anti-STEVOR IgG antibodies show differential recognition in malaria-exposed individuals

Our chemically synthesized multiepitope constructs demonstrated excellent stability and safety profiles *in silico* (Table 2), enabling robust immunological characterization. Critically, demographic analysis confirmed well-matched study groups, with no significant differences in age (Wilcoxon rank sum test, $P =$

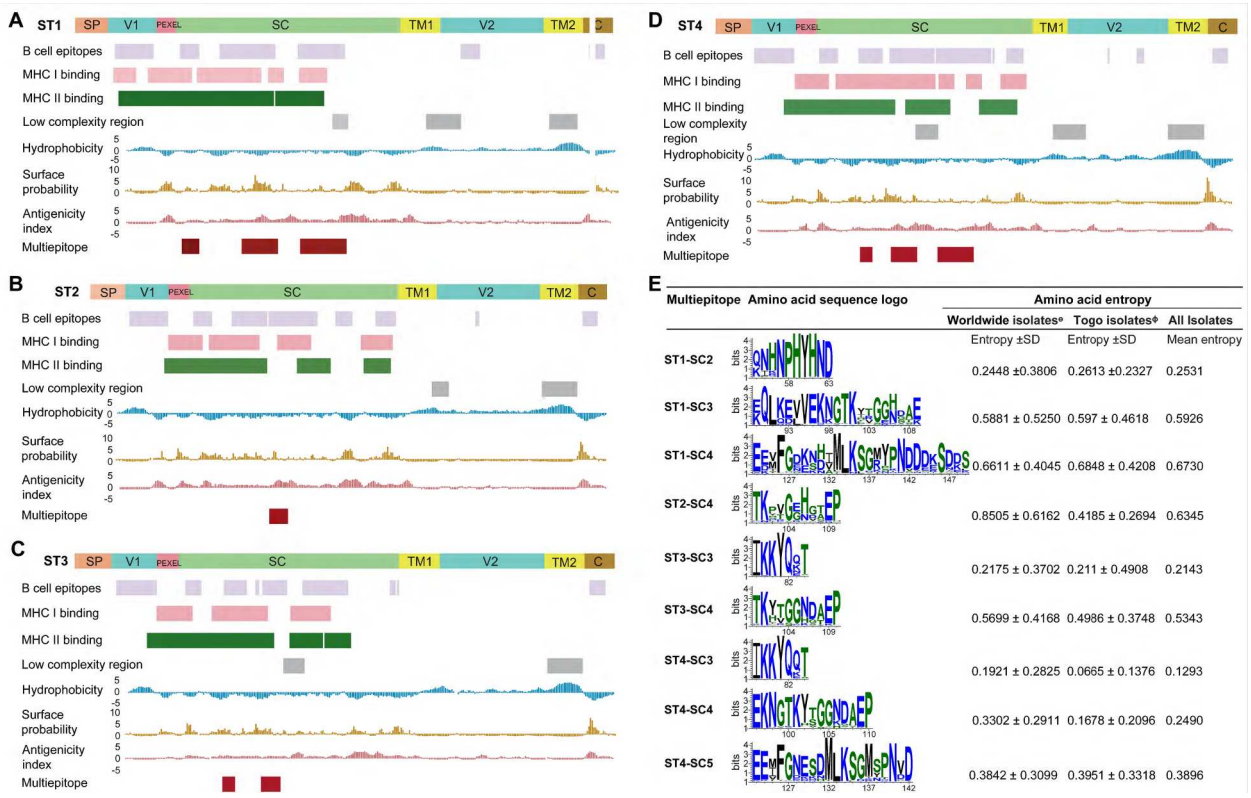

Figure 1. Mapping of domains, physicochemical characteristics, and conservation analyses of epitopes within the SC domains of STEVOR antigens. (A) Selected multiepitopes in PF3D7_1040200 (ST1). (B) Selected multiepitopes in PF3D7_0617600 (ST2). (C) Selected multiepitopes in PF3D7_0115400 (ST3). (D) Selected multiepitopes in PF3D7_0300400 (ST3). The horizontal axis of the bar graph represents the position number of the amino acid. (E) Weblogo and entropy sequences showing the amino acid sequences of the selected multiepitopes.

0.0891) or sex distribution (chi-square test, $P = 0.8676$) between severe (SMG) and (NMG) malaria cases, whereas parasite density effectively distinguished disease severity (Wilcoxon rank sum test, $P = 2.2 \times 10\text{-}16$; Table A3). The immunological assessment revealed three key findings:

Enhanced humoral recognition: NMG individuals presented significantly higher anti-multiepitope IgG levels (0.110 [IQR: 0.041–0.219]) than did those in the SMG group (0.095 [IQR: 0.028–0.170], $P = 0.003$), with both groups exceeding those of uninfected controls (NCG, Figure 2(A–D)). All the STEVOR fused multiepitopes outperformed the MSP1$_{_p83}$ control (0.014 [IQR: 0.004–0.028], Figure 2(E), Table A5).

Table 1. Amino acid conservation rate.

Multiepitopes	Isolate/ strain	AA mutation rate (%)	W-statistics	*P* value
ST1-SC2	Global	92.29	4273.5	0.58
	Togo	89.88		
ST1-SC3	Global	70.48	5161.5	0.061
	Togo	73.56		
ST1-SC4	Global	69.98	4830.5	0.3262
	Togo	72.9		
ST2-SC4	Global	60.91	6001.5	<0.001
	Togo	87.3		
ST3-SC3	Global	84.85	5041	<0.001
	Togo	88.85		
ST3-SC4	Global	67.13	5027	0.004
	Togo	73.84		
ST4-SC3	Global	94.18	5305	<0.001
	Togo	98.37		
ST4-SC4	Global	84.81	7303.5	<0.001
	Togo	95.53		
ST4-SC5	Global	84.79	5255.5	0.006

Epitope-specific patterns: The fused multiepitope ST1-Grp elicited the strongest IgG response (0.211 [IQR: 0.132-0.312], $P < 0.05$), with NMG showing superior recognition of ST1-Grp (0.235 [IQR: 0.122–0.385] vs 0.191 [IQR: 0.139–0.246], $P < 0.05$) and ST2-Grp (0.177 [IQR: 0.098–0.254] vs 0.079 [IQR: 0.044–0.119], $P < 0.001$) compared with SMG (Figure 2(F)). However, no difference in the antibody response was found for the ST2-Grp, ST3-Grp, and ST4-Grp fused multiepitopes (ST2-Grp: 0.112 [IQR: 0.068–0.195], ST3-Grp: 0.135 [IQR: 0.065–0.205], and ST4-Grp: 0.110 [IQR: 0.061–0.157], respectively). Seroprevalence varied significantly across epitopes ($\chi^2 = 14.013$, $P = 0.0029$), being highest for ST1-Grp (82.95%) and ST4-Grp (81.40%), followed by ST3-Grp (74.42%). While the seroprevalence was lowest for ST2-Grp (65.12%), it was significantly greater in the NMG group (85.71% vs 40.68%, $\chi^2 = 26.639$, $P < 0.001$) compared with the SMG group (Figure 2(G)). Further pairwise comparisons with Bonferroni-adjusted *P*-values revealed significant differences between ST1-Grp and ST2-Grp ($P = 0.011$), as well as between ST2-Grp and ST4-Grp ($P = 0.029$, Table A6).

Mutation–immunity relationship: While the amino acid mutation rate was weakly correlated with seroprevalence (Spearman correlation, $r_s = 0.114$, $P = 0.045$),

Table 2. Physicochemical properties of the fused multiepitopes and MEFA construct.

Immunogen	Theoretical **PI**	Length	Antigenicity	Allergenicity	Toxicity	GAVI	Instability index
ST1-Grp (EDVFGDKNHAMLKSGRYPNDDDESDDSQNHNPHYHNDKQLKEVVEKNGTKIRGGNSAE)	5.13	58	0.9907	Probable nonallergen	Nontoxin	-1.74	33.22
ST2-Grp (TKPVGEHGTEP)	5.37	11	0.8131	Probable nonallergen	Nontoxin	-1.391	16.19
ST3-Grp (IKKYQNTTKHVGGNDTEP)	8.44	18	0.8305	Probable nonallergen	Nontoxin	-1.639	10.48
ST4-Grp (EEIFGNESDMLKSGMSPNVDIKKYQQTEKNGTKYSGGNDAEP)	4.56	42	1.0439	Probable nonallergen	Nontoxin	-1.321	47.05
$MSP1_{-p83}$ (QIPFNLKIRANELDVLKKLVFTDPLELE)	0.7653	28	0.7653	Probable nonallergen	Nontoxin	-0.018	3.36
MEFA construct	9.58	522	0.6855	Probable nonallergen	Nontoxin	-1.169	22.61

no significant associations emerged between mutation proportion and either the antibody positivity rate (r_s = 1, $P = 0.08$) or the IgG antibody level (Table A7), suggesting functional conservation of key epitopes.

STEVOR fused multiepitopes elicit immune responses in mice

As anticipated, all immunized mice exhibited a steady increase in body weight over the course of the study, with no significant differences in baseline weight (day 0, $P = 0.312$) (Figure 3(B)). These findings suggest that neither the adjuvants nor the STEVOR-fused multiepitope vaccines induced systemic toxicity, supporting their safety profile for further evaluation.

Notably, all four experimental groups presented significantly elevated anti-STEVOR IgG antibody levels compared with both the PBS and adjuvant-only control groups ($P < 0.05$; Figure 3(C)). Strikingly, the ST1-Grp construct induced the most robust humoral immunity, with total IgG antibody titres peaking at 2.60 [IQR: 2.43–2.75] by the fourth bleed (day 42), far exceeding even the $MSP1_{\_p83}$-positive control (0.77 [IQR: 0.68–2.13]) (Figure 3(D–F), Tables A9–A10). While ST2-Grp and ST4-Grp also elicited substantial responses (reaching 1.07 [IQR: 0.27–1.84] and 0.45 [IQR: 0.27–0.55], respectively), ST3-Grp generated comparatively lower but still significant antibody levels (0.04–0.20 across timepoints). Importantly, the antibody titres in the experimental groups remained elevated throughout the final bleeding period (day 56), confirming the durability of the immune response.

In addition to humoral immunity, we observed intriguing shifts in cellular immune responses. Prior to immunization, baseline cytokine levels averaged 8.13 pg/mL (IL-2) and 33.42 pg/mL (IFN-γ). However, after the first immunization, the levels of both cytokines declined sharply (IL-2: 3.60 pg/mL; IFN-γ: 18.44 pg/mL), with further reductions after the second immunization (IL-2: 3.06 pg/mL; IFN-γ: 11.52 pg/mL) (Figure 3(G,H)). This trend persisted after the third dose (IL-2: 1.88 pg/mL; IFN-γ: 12.85 pg/mL), followed by a partial rebound after the fourth immunization (IL-2: 3.28 pg/mL; IFN-γ: 19.95 pg/mL). This biphasic cytokine profile suggests an initial immune modulation phase, potentially indicative of epitope-specific T-cell exhaustion or regulatory feedback mechanisms, warranting further mechanistic investigation.

Flow cytometry analyses revealed that, compared with PBS and the adjuvant control, the STEVOR-fused multiepitopes significantly increased both CD8 + and CD4+ T-cell proliferation ($P < 0.05$), with ST3-Grp emerging as the most immunogenic construct, resulting in the highest proportions of CD8+ (19.56%) and CD4+ T cells (54.43%) – even surpassing the $MSP1_{\_p83}$-positive control ($P < 0.05$) (Figure 4). While ST1-Grp and ST2-Grp also stimulated notable

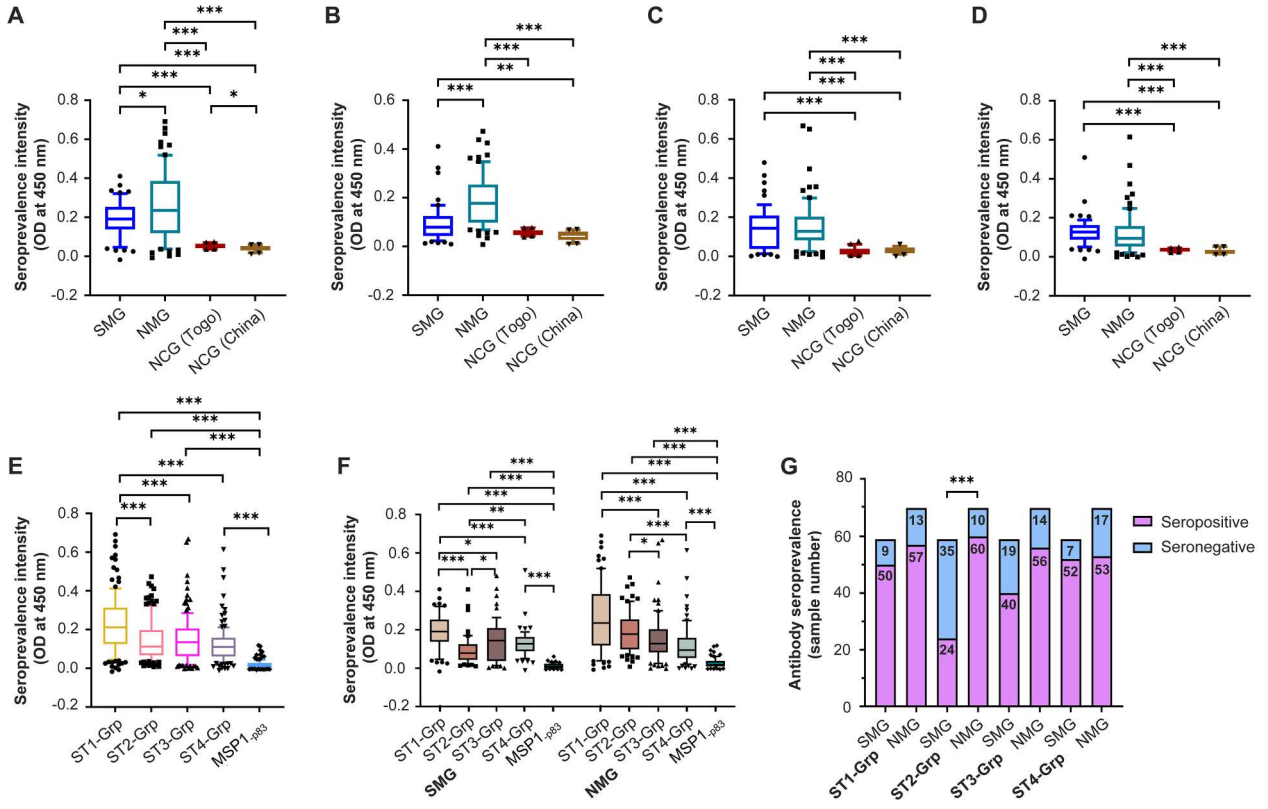

Figure 2. Differential recognition of multiepitope-specific anti-STEVOR IgG antibodies in malaria-exposed individuals. (A) Total IgG antibody recognition levels in the SMG versus the NMG to the ST1-Grp. (B) Total IgG antibody recognition levels in the SMG versus the NMG to the ST2-Grp. (C) Total IgG antibody recognition levels in the SMG versus the NMG to the ST3-Grp. (D) Total IgG antibody recognition levels in the SMG versus the NMG to the ST4-Grp. (E) Differential total IgG antibody recognition levels between ST1-Grp, ST2-Grp, ST3-Grp, ST4-Grp, and MSP1$_{_p83}$ groups. (F) Differential total IgG antibody recognition levels in the SMG versus the NMG between the ST1-Grp, ST2-Grp, ST3-Grp, and ST4-Grp groups. Seroreactivity intensity indicates the antibody levels. SMG: severe malaria group; NMG: nonsevere malaria group. NMG: Nonsevere malaria group. NCG: (uninfected) normal control group. (G) Seroprevalence of total IgG antibody recognition to STVEVOR fused multiepitopes in SMG vs NMG. The numbers on the blocks represent the number of serum samples that were seroreactive to a particular fused multiepitope. SMG: severe malaria group; NMG: nonsevere malaria group. ***: $P < 0.001$.

CD4 + expansion, the pronounced T-cell activation by ST3-Grp suggests its unique capacity to engage both cytotoxic and helper T-cell responses, a critical feature for effective vaccine-induced immunity (Figure 4(A–C)). These results imply that STEVOR multiepitopes, particularly ST3-Grp, may promote robust long-term protection by eliciting durable cellular memory, positioning them as promising candidates.

The MEFA vaccine construct demonstrated excellent structural stability and immunogenic potential through comprehensive in silico *analysis*

On the basis of the above findings that the fused multiepitopes elicit cellular and humoral immunity *in vivo*, we successfully engineered this optimized vaccine by strategically combining nine CD8+ T-cell epitopes, 11 CD4+ T-cell epitopes, and nine B-cell epitopes, via the "AAY," "GPGPG," and "KK" liners with an N-terminal adjuvant (Figure 5(A)). Structural analyses confirmed the stability of the construct, with both 2D and 3D modelling showing favourable conformations (Figure 5(B,C)), which wassupported by Ramachandran plot validation (95% residues in most favoured regions, 4.3% residues in additional allowed regions, 0.2% residues in generously allowed regions), and 0.5% in disallowed regions (Figure 5(D)). The vaccine construct exhibited ideal physicochemical properties (Table 2), passed critical safety thresholds, and was predicted to be nonallergenic and nontoxic, indicating that it is as a promising candidate for further development.

The MEFA construct demonstrated high global population coverage for CD4 + and CD8+ T-cell epitopes, achieving 97.15% overall HLA coverage

Detailed analysis revealed robust HLA-I (60.58%) and HLA-II (92.76%) specific coverage (Figure 5(F)), with optimal epitope combinations accounting for 30.48% of individuals (Figure 5(E)). Regionally, coverage was remarkably high across Africa – western Africa (98.36%), central (98.16%), and eastern (98.00%) regions

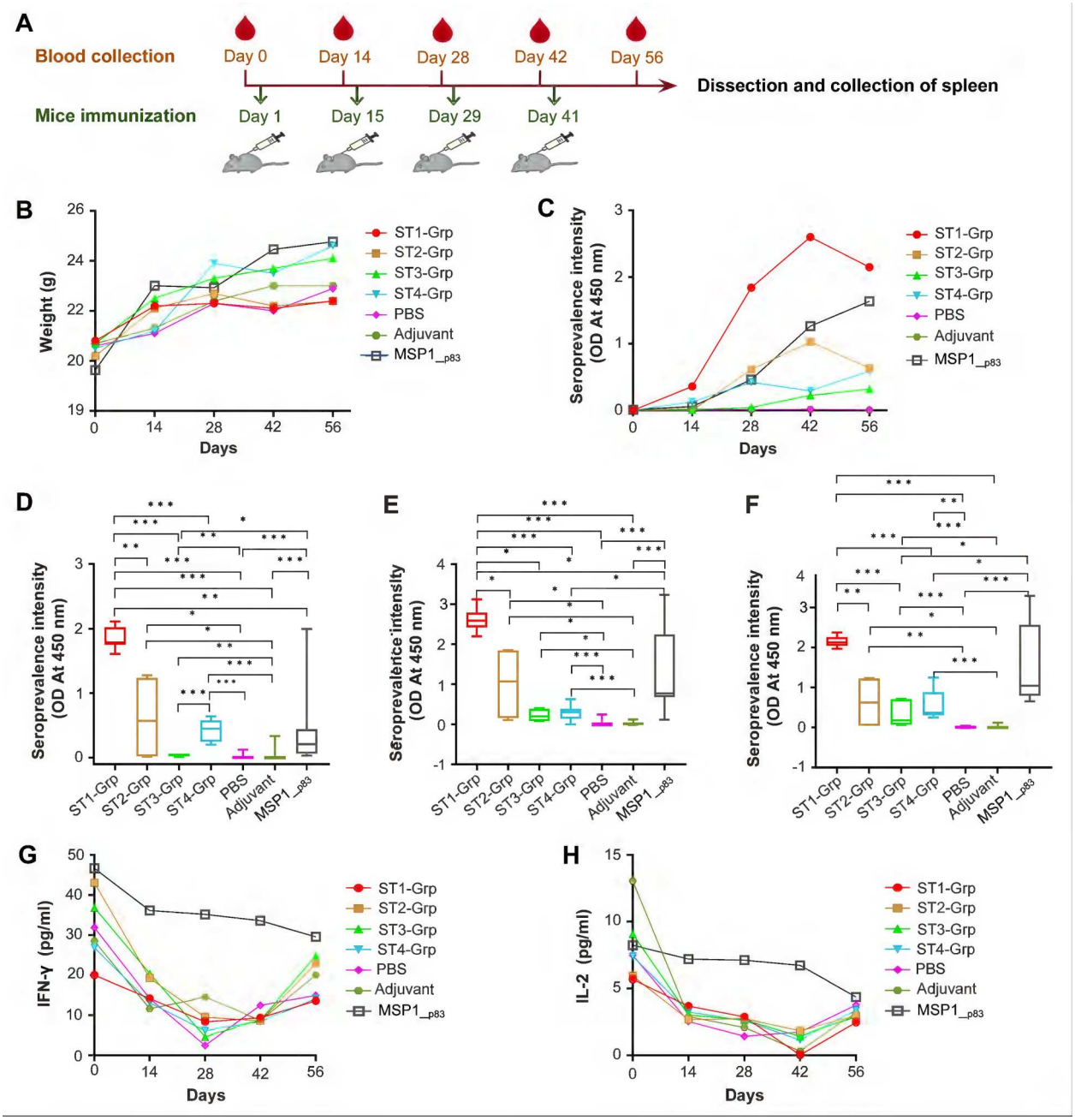

Figure 3. Levels of total IgG antibodies, IFN-γ, and IL-2 in mice immunized with the fused epitopes. (A) Schedule of mouse immunization and blood collection. (B) Changes in mouse body weight. Each point represents the mean weight of a mouse before and after blood collection. (C) Trends in the levels of IgG antibodies in the immunized following boost injections. (D) Levels of total IgG antibody in the immunized mice on day 28. (E) Levels of total IgG antibody in the immunized mice on day 42. (F) Levels of total IgG antibody in the immunized mice on day 56. (G) Trends in the levels of circulating IFN-γ following boost injections. (H) Trends in the levels of circulating IL-2 following boost injections.

presented near-universal protection potential, while northern Africa maintained strong coverage (86.44%). The only notable exception was southern Africa (62.2%), (Table A11), suggesting the the construct may require minor regional optimization whereas maintaining its excellent global protective potential.

Immune simulations revealed robust immunogenicity of the MEFA vaccine construct

Three doses progressively increased immune reactivity, with the final dose eliciting the most potent response. B cell proliferation peaked at ~60 days, whereas memory B-cells remained remarkably durable – maintaining 410 cells/mm³ even at 350 days postinjection. The cellular arm showed vigorous activity, with the number of CD8+ T cells increasing to 1080 cells/mm³ by day 13 and the number of memory CD4+ T cells increasing at 1890 cells/mm³. Antibody production surged to ~225,700 (IgM + IgG) by day 65, indicating effective humoral immunity. Notably, the cytokine responses were exceptionally strong, with the level of IFN-γ reaching 427,000 ng/mL and the level of IL-2 peaking at 478,000 ng/mL (Figure S5), confirming the ability

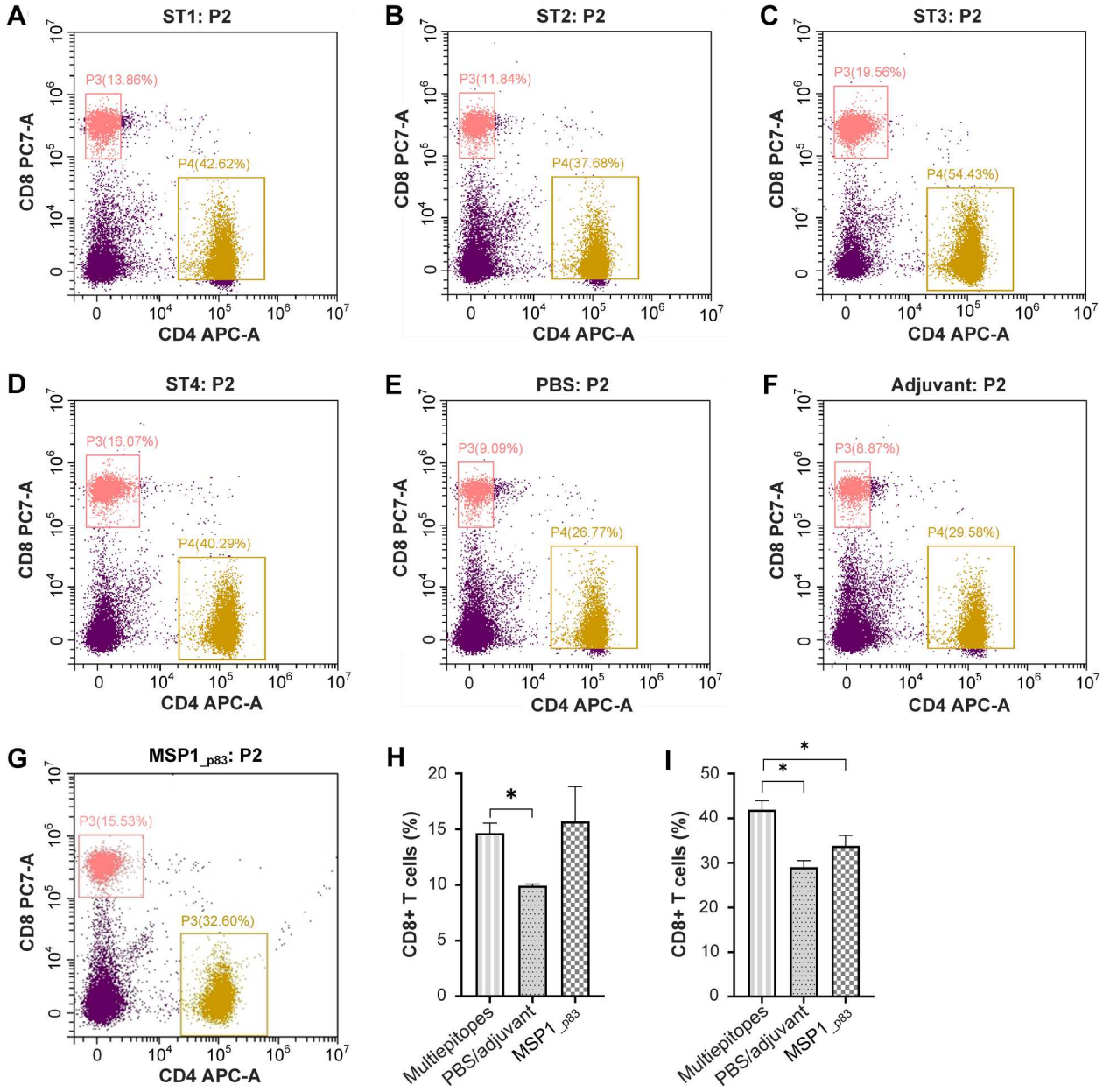

Figure 4. Levels of CD8+ T- and CD4+ T-cell proliferation in the spleens of immunized mice. (A-G) Proportion of both CD4+ T and CD8+ T cells in mice immunized with ST1-Grp, ST2-Grp, ST3-Grp, ST4-Grp, PBS control, adjuvant control, MSP1$_{_p83}$ control groups. P3 represents the proportion of CD8+ T cells. P4 represents the proportion of CD4+ T cells. (H) Proportion of CD8+ T cells in mice immunized with ST1-Grp, ST2-Grp, ST3-Grp, ST4-Grp, PBS/adjuvant control, and MSP1$_{_p83}$ positive control groups. (I) Proportion of CD4+ T cells in immunized mice with ST1-Grp, ST2-Grp, ST3-Grp, ST4-Grp, PBS/adjuvant control, and MSP1$_{_p83}$ positive control groups.

of the construct to stimulate robust Th1-type immunity. These results collectively highlight the capacity of the MEFA vaccine to induce comprehensive, long-lasting immune protection patterns.

Expression, purification, and clinical immunogenicity evaluation of the MEFA vaccine construct

The MEFA and MSP1$_{-42}$ positive control (NCBI accession no. XP_001352170) proteins were successfully expressed in soluble form using *E. coli* BL21(DE3) and purified via Ni^{2}+ affinity chromatography. SDS-PAGE analysis revealed single, sharp bands at 58 kDa (MEFA) and 44 kDa (MSP1$_{-42}$) without degradation products (Figure 6(A)), confirming high purity. Western blot analysis with an anti-His antibody revealed strong immunoreactive bands at the predicted molecular weights (Figure 6(B)). These results demonstrate that both the MEFA and MSP1$_{-42}$ proteins were successfully expressed and purified in soluble form with preserved antigenicity.

Clinical serum analysis revealed distinct immunogenicity profiles. While MSP1$_{-42}$ elicited higher overall total IgG antibody responses (0.290 [IQR:0.072-0.741]) than did MEFA (0.147 [0.061-0.277], $P = 2.6 \times 10^{-4}$; Figure 6(C)), MEFA elicited significantly greater anti-MEFA IgG levels in the nonsevere malaria groups

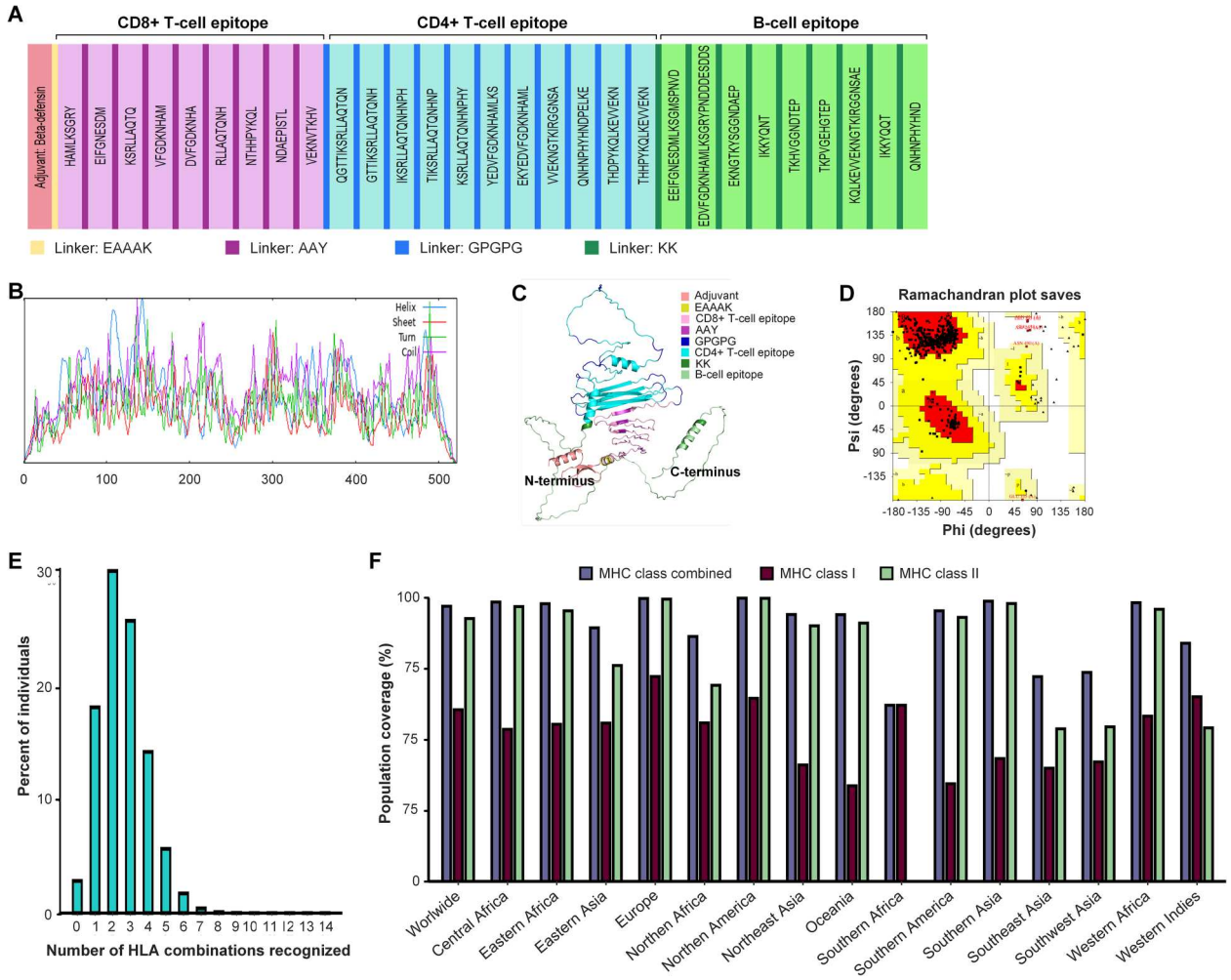

Figure 5. Multiepitope fusion antigen (MEFA) vaccine construct and population coverage of T-cell epitopes. (A) MEFA construct consisting of adjuvant, CD8 + and CD4+ T-cell epitopes, B-cell epitopes and linkers. (B) Two-dimensional structural model of the MEFA construct. (C) Three-dimensional structural model of the MEFA construct. (D) Ramachandran plot of the MEFA construct. Residues in most favoured regions [A, B, L]. Residues in additional allowed regions [a, b, l, p]. Residues in generously allowed regions [~a, ~b, ~l, ~p]. (E) Number of HLA combinations recognized by different percentages of individuals globally. (F) Population coverage of the individual classes and combined classes worldwide.

(NMG:0.169 [0.097–0.276] vs SMG:0.087 [0.050-0.262], $P = 0.029$; Figure 6(D, E)). Importantly, the seroprevalence of the MEFA was 82.9% in the NMG group versus 66.1% in the SMG group ($P = 0.046$; Figure 6(G)), suggesting its potential immunogenicity.

Structural analysis confirms the immunogenic potential of MEFA through stable HLA-II and TCR interactions

Molecular docking revealed strong binding between MEFA and HLA-II, with favourable binding energies of −15.1 kcal/mol (α-chain) and −12.6 kcal/mol (β-chain), indicating stable complex formation. Furthermore, the MEFA-HLA-II complex effectively engaged the TCR, exhibiting binding energies of −8.4 kcal/mol (TCR β-chain) and −2.6 kcal/mol (TCR α-chain), supporting its potential for T-cell recognition. Key interacting residues at these interfaces (Figure S6) further validated the structural compatibility of MEFA with the immune recognition machinery, reinforcing its potential as a vaccine candidate capable of eliciting robust cellular immunity.

Discussion

Computational immunology is currently being used to identify epitopes of various pathogen antigens, including malaria antigens, and to design multiepitope constructs [36–39]. However, several of those studies were limited in evaluating either the *in vitro* or *in vivo* antigenicity and immunogenicity of these constructs.

Recent studies revealed that the SC domains of STEVORs were serorecognized and exhibited differential seroreactivity between children and adults exposed to *P. falciparum* infections in areas where malaria is endemic [12]. The SC domain of STEVORs exposed on the iRBC surface elicits protective IgG antibodies that are able to reduce the formation of rosetting [18]. These findings raised questions about epitope immunogens in the SC domain of STEVORs.

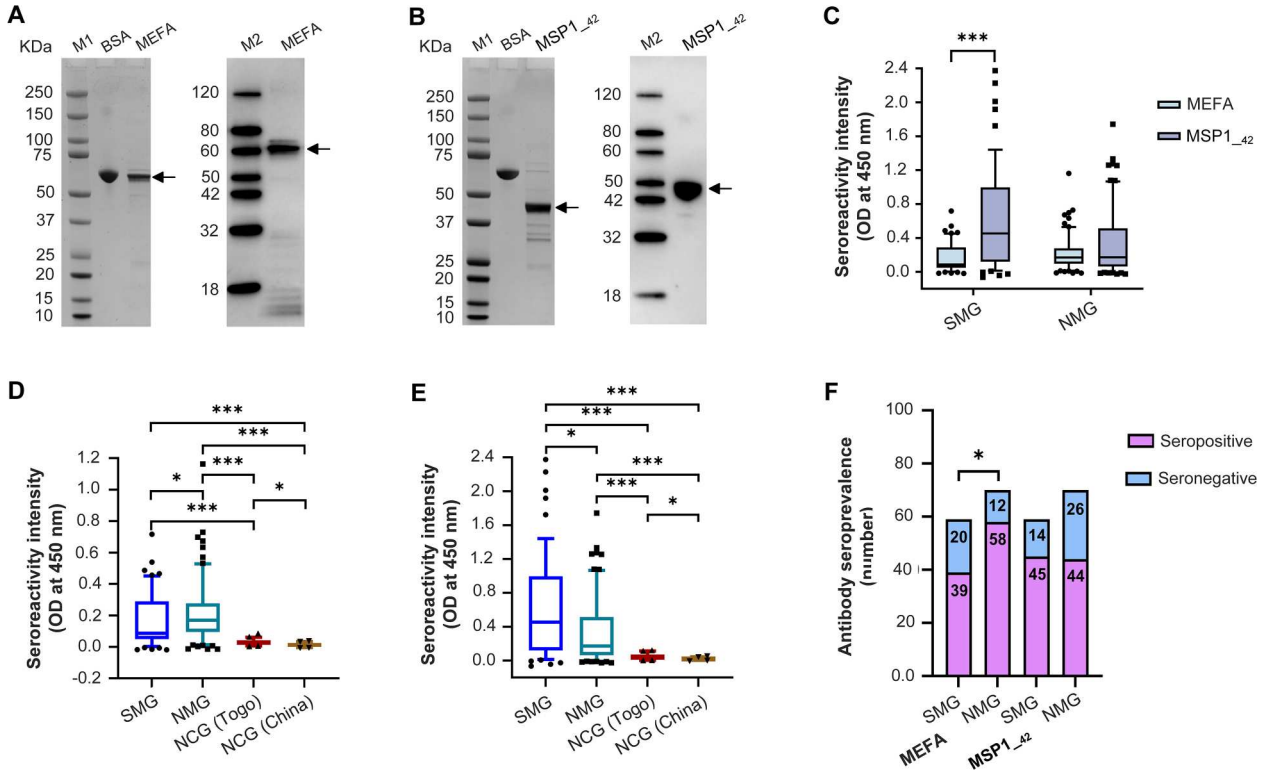

Figure 6. Differential recognition of MEFA-specific anti-STEVOR IgG antibodies in malaria-exposed individuals. Recombinant MEFA (A) and MSP1$_{-42}$ (B) proteins expressed in *E. coli* and purified via Ni^{2+} affinity chromatography. SDS-PAGE analysis was performed to assess protein purity (left). Lane M1: molecular weight marker (kDa); Lane BSA: bovine serum albumin control. Western blotting with anti-His antibody was used to confirm protein identity (right). Lane M2: Western blot marker. Arrows indicate the expected positions of MEFA and MSP1$_{-42}$ proteins. (C) Differential total IgG antibody recognition levels in the SMG versus the NMG between the MEFA, and MSP1$_{-42}$. (D) Differential total IgG antibody recognition levels in the SMG versus the NMG to the MEFA. (E) Total IgG antibody recognition levels in the SMG versus the NMG to the MSP1$_{-42}$. (F) Seroprevalence of IgG antibody recognition in SMG vs NMG to MEFA and MSP1$_{-42}$.

The precise domain mapping of the four STEVOR antigens enabled strategic selection of the SC region as our target for multiepitope identification – a foundation for constructing a balanced conservation for broad coverage with variability in the immune response [12,18].

Our analysis revealed multifunctional recognition multiepitopes that overlap T-cell epitopes (both MHC I and II-restricted) and either linear or conformational B-cell epitopes [23]. Each multiepitope demonstrated: (1) optimal vaccine characteristics with strong predicted antigenicity [40], (2) dual recognition capability through overlapping T-cell (both MHC I/II-restricted) and B-cell (linear/conformational) epitope sites; (2) [41], (3) broad population coverage through binding to diverse HLA alleles [42], and nontoxicity/nonallergenicity, positioning the SC domain multiepitopes as strategic targets for a STEVOR multiepitope vaccine. Globally, the average combined HLA class coverage (86.48%) for the multiepitopes in this study was greater than that reported for other epitopes in previous studies (83.48%) [36]. The population coverage of class II HLA types was generally lower than that of class I HLA types, with no class II coverage reported in the southern African population, which is consistent with previous studies [38]. Exploring more extensive HLA class II typing efforts across diverse southern African populations is necessary to better understand allele distributions [43].

Our comprehensive conservation analysis demonstrated strong conservation of the selected multiepitopes across *P. falciparum* 3D7 isolates and global strains (AA sequence entropy <0.5) [44], suggesting structural or functional constraints for suitability as vaccine candidates. This evidence is also reflected in sequence weblogo and mutation rate analyses whose results aligned one to another [45] The average AA conservation rate of all the multiepitopes was higher (>85% vs 80%) in *P. falciparum* Togo clinical isolates than in global strains, with two STEVOR multiepitopes (ST4-SC3 and ST4-SC4) > 98% exceptionally conserved, suggesting a balanced immunogenicity.

Chemically synthesized multiepitope constructs demonstrated excellent stability and safety profiles *in silico*, and enabled robust immunological characterization in the sera of *P. flaciparum*-exposed individuals. The multiepitopes enhanced humoral recognition (significantly greater in the sera from NMG individuals than in those from the SMG group), with epitope-specific patterns (ST1-Grp elicited the strongest

response). Notably, while the AA mutation rate was weakly correlated with seroprevalence, no significant associations emerged between mutation proportion and either antibody positivity ($P = 0.08$) or IgG levels, suggesting functional conservation of key epitopes. The differential recognition patterns, particularly the superior responses in NMG, suggest the potential immunogenicity of these multiepitopes.

Although mice are not natural hosts for *Plasmodium falciparum*, we used BALB/c mice in this study as a well-established model for proof-of-concept immunogenicity and safety evaluation *in vivo*. All immunized mice exhibited a steady increase in body weight over the course of the study, confirming that the multiepitope-based vaccine formulations were well-tolerated, with no overt signs of toxicity or morbidity. STEVOR-specific IgG antibody responses were potent and sustained in the experimental groups following immunization, demonstrating a strong humoral immune response, which is consistent with previous studies that used *Plasmodium* immunogens [46]. We also found a progressive decline in the levels of circulating IL-2 and IFN-γ in the serum of mice with increasing booster injections. This decrease may be related to several factors, including limitations in the mouse model, and the activation of regulatory T cells (Tregs), which can inhibit the function of effector T cells, resulting in a decrease in the production of cytokines. Following induction of the immune response, there is usually a feedback mechanism that downregulates the production of cytokines to prevent excessive activation and potential tissue damage [47]. IL-2 and IFN-γ usually peak within 48–72 h after injection. Over time (usually within 72 h to one week after injection), the levels of IL-2 and IFN-γ begin to decrease, which may be related to the regulatory mechanism of the immune response, including factors such as the activation of Tregs and cytokine feedback inhibition [48].

Flow cytometry analyses revealed increases in the numbers of CD4 + T and CD8 + T cells in the spleen, confirming enhanced cellular immunity. This evidence aligns with the above findings on humoral responses, suggesting that these multiepitopes could stimulate the immune system in mice, resulting in the proliferation of immune cells. Collectively, these data demonstrate that STEVOR fused multiepitopes effectively stimulate both humoral and cellular immunity, highlighting their potential as promising vaccine candidates warranting further development. These findings align with the knowledge that cell-mediated immunity is driven mainly by T cells, especially CD8 + T and CD4+ T cells, which usually occur early in the infection process [49]. Humoral immunity involves B cells producing antibodies in response to extracellular antigens, which usually occurs after the initial cellular immune response and takes longer to develop [50].

On the basis of the above results, we rationally designed a multiepitope fusion antigen (MEFA) vaccine construct following previous studies [36–39]. The MEFA construct comprises all the fused multiepitopes, the beta-defensin-3 adjuvant at the N-terminus, and linkers [51–57]. The MEFA vaccine construct, with a molecular weight of 57.02 kDa, demonstrated excellent structural stability and immunogenic potential through comprehensive *in silico* analysis [58,59], with a half-life of more than 10, 20, and 30 h in *E. coli*, yeast cells, and mammalian reticulocytes, respectively. This result is satisfactory considering that a longer half-life of a vaccine will remain intact for an extended period, thereby increasing the chances of inducing an effective immune response [60,61]. Notably, it demonstrated exceptional global population coverage for both CD4 + and CD8+ T-cell epitopes, achieving an outstanding 97.15% overall HLA coverage. Regionally, coverage was remarkably high across Africa – western (98.36%), central (98.16%), and eastern (98.00%) regions presented near-universal protection potential, which is consistent with the geographical prevalence of *P. falciparum* malaria.

Immune simulations of the MEFA construct revealed a significant immune response involving T cells and B cells and demonstrated strong and sustained activation of both humoral and cellular immune responses. These results are consistent with those reported in previous studies that assessed the immunogenicity of multiepitope vaccine constructs *in silico* [37, 62].

The 42 kDa fragment of *P. falciparum* merozoite surface protein 1 ($MSP1_{-42}$) plays a critical role in erythrocyte invasion by binding heparin-like molecules on erythrocytes [63], and it elicits strong antibody responses in infected individuals [64]. In this study, $MSP1_{-42}$ served as a benchmark for evaluating the immunoreactivity of our novel MEFA construct. While $MSP1_{-42}$-specific IgG levels were higher overall, they were significantly elevated in severe malaria cases (SMG) compared to nonsevere cases (NMG). Conversely, NMG patients exhibited stronger MEFA-specific IgG responses and higher seroprevalence rates, suggesting that MEFA may induce protective immunity associated with milder disease outcomes. This dichotomy highlights MEFA's potential as a vaccine candidate that could skew immunity toward protective rather than pathogenic responses.

Unlike multiepitope vaccines that target Toll-like receptors (TLRs), which lack direct roles in antigen presentation or adaptive immunity [65–67], our MEFA construct leverages epitopes from STEVOR proteins. These antigens are processed by APCs and presented via MHC class II to activate CD4+ T cells [68]. By focusing on HLA-DRB1*04:01, a haplotype

linked to severe malaria [34], we demonstrated high-affinity binding of MEFA to MHC II (negative free energy) and subsequent docking with the TCR. This structural compatibility underscores the capacity of MEFA to drive CD4+ T-cell responses, aligning with adaptive immunity mechanisms and offering a more biologically rational design than TLR-dependent approaches.

Limitations and future directions

In this study, the levels of IL-2 and IFN-γ in serum (not antigen-stimulated splenocyte cultures) were measured as systemic indicators of vaccine-induced immune activation. While these circulating cytokines reflect broader immunogenicity, we fully acknowledge that antigen-specific T-cell responses (e.g. via *ex vivo* restimulation assays) would provide more mechanistic insight. A further limitation is that our flow cytometry analysis focused solely on phenotyping total CD4 and CD8 T-cell counts of the spleen in a mouse model without antigen stimulation (e.g. evaluation of antigen-specific T cells) to test functional responses. While these data provide foundational insights into T-cell populations, we acknowledge that antigen-specific functional assays (e.g. via ELISpot or flow cytometry with STEVOR probes) and the evaluation of memory B-cell reactivity (e.g. STEVOR-specific plasmablasts or IgG + B cells), remain essential for understanding humoral immunity and will be prioritized in future work.

This study systematically demonstrated the promise of the MEFA vaccine construct through: (1) *in silico* validation of immunogenicity, including immune simulation and molecular docking of the MEFA-HLA complex with T-cell receptors, confirming its structural compatibility for robust T-cell activation; and (2) experimental validation via recombinant expression and *ex vivo* assessment, revealing significantly higher anti-MEFA IgG levels in nonsevere versus severe malaria cases ($P < 0.05$). This finding aligns with emerging evidence linking targeted immune responses to improved clinical outcomes. While these results establish compelling antigenicity and mechanistic potential, we emphasize that antigen-specific T cell response and Fc-mediated effector functions (e.g. opsonic phagocytosis) definitive validation and protective efficacy studies – including Fc-mediated effector function (e.g. opsonic phagocytosis)-controlled animal challenge trials and phased clinical testing – represent the essential next steps to translate MEFA from the bench to the bedside. Such studies will rigorously evaluate the correlations between immune parameters (e.g. IgG titre and T-cell responses) and clinical protection, ultimately validating potential of MEFA as a next-generation malaria vaccine candidate.

Conclusion

To our knowledge, this study represents the first rational design of a fusion antigen vaccine (MEFA) leveraging conserved, nonallergenic, and highly immunogenic multiepitopes from *P. falciparum* STEVORs – demonstrating broad immunogenicity while maintaining safety and antigenic specificity. Our findings establish a compelling proof-of-concept for the antigenicity and mechanistic potential of MEFA. The critical next steps should focus on: (1) definitive validation of antigen-specific T-cell responses and Fc-mediated effector functions to elucidate immune correlates of protection, and (2) rigorous protective efficacy studies in preclinical models/clinical trials. These essential investigations will bridge our promising *in silico* and *ex vivo* results with clinical application, ultimately positioning MEFA as a next-generation vaccine candidate for severe malaria.

Acknowledgements

The authors wish to acknowledge the ChinaPeptides, QYAOBIO (Shanghai, China) for epitope synthesis.

Authors' contributions

Zhi-Shan Sun: Methodology, Investigation, Visualization, Data curation, Formal analysis, Validation. Writing – original draft, Writing – review & editing. Jing-Xian Yin: Methodology, Formal analysis, Data curation. Han-Qing Zhao: Methodology, Data curation. Yin-Shan Zhu: Methodology, Investigation. Shen-Bo Chen: Investigation, Resources. Hai-Mo Shen: Data curation, Resources. Bin-Xu: Resources, Investigation. Xiao-Nong Zhou: Writing – review & editing. Tian-Yu Wang: Investigation. Wan-Xuan Yang: Investigation. Yi-Wen Duan: Investigation. Jun-Hu Chen: Writing – review & editing, supervision, funding acquisition. Kokouvi Kassegne: Conceptualization, Resources, Methodology, Validation, Writing – review & editing, Supervision, Project administration.

Disclosure statement

Kokouvi Kassegne, Jun-Hu Chen, Zhi-Shan Sun, and Xiao-Nong Zhou have a patent related to this article (application number 2025108602394).

Funding

This study was financially supported in part the Natural Science Foundation of Shanghai (Grant No. 24ZR1473200), a grant from the Bill & Melinda Gates Foundation (Grant No. INV-003421) the National Key Research and Development Program of China (2018YFE0121600), and the Shanghai Jiao Tong University Global Strategic Partnership Fund (KJ3-0204-23-0001). The sponsor played no role in the study design; in the collection, analysis, or interpretation of the

data; in the writing of the report; or in the decision to submit the article for publication.

Availability of data and materials

The original contributions presented in the study are included in the article and supplementary data. Further inquiries can be directed to the corresponding authors.

ORCID

Kokouvi Kassegne http://orcid.org/0000-0002-7067-177X

References

[1] World Health Organization. World malaria report 2024: addressing inequity in the global malaria response. Geneva: World Health Organization2024.

[2] Kassegne K, Abe EM, Cui YB, et al. Contribution of *Plasmodium immunomics*: potential impact for serological testing and surveillance of malaria. Expert Rev Proteomics. 2019 Feb;16(2):117–129. doi:10.1080/14789450.2019.1554441

[3] World Health Organization. World malaria report 2015 2015 [cited 2024 Jun 19]. Available from: https://www.who.int/publications/i/item/9789241565158.

[4] Wahlgren M, Goel S, Akhouri RR. Variant surface antigens of *Plasmodium falciparum* and their roles in severe malaria. Nat Rev Microbiol. 2017/08/01;15(8):479–491. doi:10.1038/nrmicro.2017.47

[5] Gardner MJ, Hall N, Fung E, et al. Genome sequence of the human malaria parasite *Plasmodium falciparum*. Nature. 2002 Oct 3;419(6906):498–511. doi:10.1038/nature01097

[6] Lavstsen T, Turner L, Saguti F, et al. *Plasmodium falciparum* erythrocyte membrane protein 1 domain cassettes 8 and 13 are associated with severe malaria in children. Natl Acad Scie USA. 2012;109(26):E1791–E1800. doi:10.1073/pnas.1120455109

[7] Niang M, Bei AK, Madnani KG, et al. STEVOR is a *Plasmodium falciparum* erythrocyte binding protein that mediates merozoite invasion and rosetting. Cell Host Microbe. 2014 Jul 9;16(1):81–93. doi:10.1016/j.chom.2014.06.004

[8] Goel S, Palmkvist M, Moll K, et al. RIFINs are adhesins implicated in severe *Plasmodium falciparum* malaria. Nat Med. 2015/04/01;21(4):314–317. doi:10.1038/nm.3812

[9] Rasti N, Wahlgren M, Chen Q. Molecular aspects of malaria pathogenesis. FEMS Immunol Med Microbiol. 2004 May 1;41(1):9–26. doi:10.1016/j.femsim.2004.01.010

[10] Doumbo OK, Thera MA, Koné AK, et al. High levels of *Plasmodium falciparum* rosetting in all clinical forms of severe malaria in African children. Am J Trop Med Hyg. 2009 Dec;81(6):987–993. doi:10.4269/ajtmh.2009.09-0406

[11] Sanyal S, Egée S, Bouyer G, et al. *Plasmodium falciparum* STEVOR proteins impact erythrocyte mechanical properties. Blood. 2012 Jan 12;119(2):e1–e8. doi:10.1182/blood-2011-08-370734

[12] Zhou AE, Berry AA, Bailey JA, et al. Antibodies to peptides in semiconserved domains of RIFINs and STEVORs correlate with malaria exposure. mSphere. 2019 Mar 20;4(2):e00097-19. doi:10.1128/mSphere.00097-19

[13] Bachmann A, Scholz JA, Janßen M, et al. A comparative study of the localization and membrane topology of members of the RIFIN, STEVOR and PfMC-2TM protein families in *Plasmodium falciparum*-infected erythrocytes. Malar J. 2015 Jul 16;14:274. doi:10.1186/s12936-015-0784-2

[14] Wichers JS, Scholz Judith AM, Strauss J, et al. Dissecting the gene expression, localization, membrane topology, and function of the *Plasmodium falciparum* STEVOR Protein Family. mBio. 2019;10(4):e01500-19. doi:10.1128/mbio.01500-19

[15] Travassos MA, Niangaly A, Bailey JA, et al. Children with cerebral malaria or severe malarial anaemia lack immunity to distinct variant surface antigen subsets. Sci Rep. 2018 2018/04/19;8(1):6281. doi:10.1038/s41598-018-24462-4

[16] Salanti A, Dahlbäck M, Turner L, et al. Evidence for the involvement of VAR2CSA in pregnancy-associated malaria. J Exp Med. 2004 Nov 1;200(9):1197–1203. doi:10.1084/jem.20041579

[17] Doritchamou JYA, Morrison R, Renn JP, et al. Placental malaria vaccine candidate antigen VAR2CSA displays atypical domain architecture in some *Plasmodium falciparum* strains. Commun Biol. 2019/12/06;2(1):457. doi:10.1038/s42003-019-0704-z

[18] Niang M, Yam Y, Preiser X, et al. The *Plasmodium falciparum* STEVOR multigene family mediates antigenic variation of the infected erythrocyte. PLoS Pathog. 2009 Feb;5(2):e1000307. doi:10.1371/journal.ppat.1000307

[19] Kassegne K, Koukoura K, Shen K, et al. Genome-wide analysis of the malaria parasite *Plasmodium falciparum* isolates from Togo reveals selective signals in immune selection-related antigen genes. Front Immunol. 2020;11:552698. doi:10.3389/fimmu.2020.552698

[20] Kassegne K, Fei SW, Ananou K, et al. A molecular investigation of malaria infections from high-transmission areas of southern Togo reveals different species of *Plasmodium* parasites. Front Microbiol. 2021;12:732923. doi:10.3389/fmicb.2021.732923

[21] Nevagi RJ, Toth I, Skwarczynski M. 12 – Peptide-based vaccines. In: Koutsopoulos S, editors. Peptide applications in biomedicine, biotechnology and bioengineering. Brisbane (QLD): Woodhead Publishing; 2018. p. 327–358.

[22] Haste Andersen P, Nielsen M, Lund O. Prediction of residues in discontinuous B-cell epitopes using protein 3D structures. Protein Sci: Publ Protein Soc. 2006 Nov;15(11):2558–2567. doi:10.1110/ps.062405906

[23] Reynisson B, Alvarez B, Paul S, et al. NetMHCpan-4.1 and NetMHCIIpan-4.0: improved predictions of MHC antigen presentation by concurrent motif deconvolution and integration of MS MHC eluted ligand data. Nucleic Acids Res. 2020;48(W1):W449–W454. doi:10.1093/nar/gkaa379

[24] Blank A, Fürle K, Jäschke A, et al. Immunization with full-length *Plasmodium falciparum* merozoite surface protein 1 is safe and elicits functional cytophilic antibodies in a randomized first-in-human trial. npj Vaccines. 2020/01/31;5(1):10. doi:10.1038/s41541-020-0160-2

[25] Lopera-Mesa TM, Doumbia S, Konaté D, et al. Effect of red blood cell variants on childhood malaria in Mali: a prospective cohort study. Lancet Haematol. 2015;2(4):e140–e149. doi:10.1016/S2352-3026(15)00043-5

[26] Severe malaria. Trop Med Int Health. 2014 Sep;19(Suppl 1):7–131.
[27] World Health Organization. Malaria 2023 [cited 2024 Jun 19]. Available from: https://www.who.int/news-room/fact-sheets/detail/malaria.
[28] Uwase J, Chu R, Kassegne K, et al. Immunogenicity analysis of conserved fragments in *Plasmodium ovale* species merozoite surface protein 4. Malar J. 2020 Mar 30;19(1):126. doi:10.1186/s12936-020-03207-7
[29] Xu Q, Liu S, Kassegne K, et al. Genetic diversity and immunogenicity of the merozoite surface protein 1 C-terminal 19-kDa fragment of *Plasmodium ovale* imported from Africa into China. Parasit Vectors. 2021 Nov 24;14(1):583. doi:10.1186/s13071-021-05086-6
[30] Shen FH, Ong JJY, Sun YF, et al. A chimeric *Plasmodium vivax* merozoite surface protein antibody recognizes and blocks erythrocytic *P. cynomolgi* Berok merozoites in vitro. Infect Immun. 2021 Jan 19;89(2): e00645-20. doi:10.1128/IAI.00645-20.
[31] Pulendran B, Arunachalam S, O'Hagan DT. Emerging concepts in the science of vaccine adjuvants. Nat Rev Drug Discovery. 2021/06/01;20(6):454–475. doi:10.1038/s41573-021-00163-y
[32] Singh A, Thakur M, Sharma LK, et al. Designing a multiepitope peptide based vaccine against SARS-CoV-2. Sci Rep. 2020/10/01;10(1):16219. doi:10.1038/s41598-020-73371-y
[33] Abramson J, Adler J, Dunger J, et al. Accurate structure prediction of biomolecular interactions with AlphaFold 3. Nature. 2024/06/01;630(8016):493–500. doi:10.1038/s41586-024-07487-w
[34] Osafo-Addo AD, Koram KA, Oduro AR, et al. HLA-DRB1*04 allele is associated with severe malaria in northern Ghana. Am J Trop Med Hyg. 2008 Feb;78(2):251–255. doi:10.4269/ajtmh.2008.78.251
[35] Yin Y, Wang XX, Mariuzza RA. Crystal structure of a complete ternary complex of T-cell receptor, peptide – MHC, and CD4. Proc Natl Acad Sci USA. 2012 2012/04/03;109(14):5405–5410. doi:10.1073/pnas.1118801109
[36] Bemani P, Amirghofran Z, Mohammadi M. Designing a multiepitope vaccine against blood-stage of *Plasmodium falciparum* by in silico approaches. J Mol Graphics Modell. 2020 Sep;99:107645. doi:10.1016/j.jmgm.2020.107645
[37] Atapour A, Vosough P, Jafari S, et al. A multiepitope vaccine designed against blood-stage of malaria: an immunoinformatic and structural approach. Sci Rep. 2022 2022/07/08;12(1):11683. doi:10.1038/s41598-022-15956-3
[38] Maharaj L, Adeleke VT, Fatoba AJ, et al. Immunoinformatics approach for multiepitope vaccine design against *P. falciparum* malaria. Infect Genet Evol: J Mol Epidemiol Evol Genet Infect Dis. 2021 Aug;92:104875. doi:10.1016/j.meegid.2021.104875
[39] Pandey RK, Bhatt TK, Prajapati VK. Novel immunoinformatics approaches to design multiepitope subunit vaccine for malaria by investigating anopheles salivary protein. Sci Rep. 2018 2018/01/18;8(1):1125. doi:10.1038/s41598-018-19456-1
[40] Doytchinova IA, Flower DR. VaxiJen: a server for prediction of protective antigens, tumour antigens and subunit vaccines. BMC Bioinformatics. 2007 Jan 5;8:4. doi:10.1186/1471-2105-8-4
[41] Bui HH, Sidney J, Dinh K, et al. Predicting population coverage of T-cell epitope-based diagnostics and vaccines. BMC Bioinformatics. 2006 Mar 17;7:153. doi:10.1186/1471-2105-7-153
[42] Shukla P, Pandey P, Prasad B, et al. Immuno-informatics analysis predicts B and T cell consensus epitopes for designing peptide vaccine against SARS-CoV-2 with 99.82% global population coverage. Brief Bioinform.. 2022 Jan 17;23(1):bbab496. doi:10.1093/bib/bbab496
[43] Sullivan JS. HLA types in South Africa. Nat Med. 2000/01/01;6(1):3–3. doi:10.1038/71513
[44] Strait BJ, Dewey TG. The Shannon information entropy of protein sequences. Biophys J. 1996 Jul;71(1):148–155. doi:10.1016/S0006-3495(96)79210-X
[45] Harrison TE, Mørch AM, Felce JH, et al. Structural basis for RIFIN-mediated activation of LILRB1 in malaria. Nature. 2020 Nov;587(7833):309–312. doi:10.1038/s41586-020-2530-3
[46] Ge J, Wang Q, Chen G, et al. Immunogenicity and antigenicity of a conserved fragment of the rhoptry-associated membrane antigen of *Plasmodium vivax*. Parasit Vectors. 2022 2022/11/15;15(1):428. doi:10.1186/s13071-022-05561-8
[47] Sojka DK, Bruniquel D, Schwartz RH, et al. IL-2 secretion by CD4+ T cells in vivo is rapid, transient, and influenced by TCR-specific competition. J Immunol (Baltimore, Md: 1950). 2004 May 15;172(10):6136–6143. doi:10.4049/jimmunol.172.10.6136
[48] Shimizu K, Fields RC, Giedlin M, et al. Systemic administration of interleukin 2 enhances the therapeutic efficacy of dendritic cell-based tumor vaccines. Proc Natl Acad Sci U S A. 1999 Mar 2;96(5):2268–2273. doi:10.1073/pnas.96.5.2268
[49] Sun L, Su Y, Jiao A, et al. T cells in health and disease. Signal Transduct Target Ther. 2023/06/19;8(1):235. doi:10.1038/s41392-023-01471-y
[50] Cyster JG, Allen CDC. B cell responses: cell interaction dynamics and decisions. Cell. 2019;177(3):524–540. doi:10.1016/j.cell.2019.03.016
[51] Weinberg A, Jin G, Sieg S, et al. The yin and yang of human Beta-defensins in health and disease. Front Immunol. 2012;3:294. doi:10.3389/fimmu.2012.00294
[52] Ferris LK, Mburu YK, Mathers AR, et al. Human beta-defensin 3 induces maturation of human langerhans cell-like dendritic cells: an antimicrobial peptide that functions as an endogenous adjuvant. J Invest Dermatol. 2013 Feb;133(2):460–468. doi:10.1038/jid.2012.319
[53] Chen X, Zaro JL, Shen WC. Fusion protein linkers: property, design and functionality. Adv Drug Delivery Rev. 2013 Oct;65(10):1357–1369. doi:10.1016/j.addr.2012.09.039
[54] Yang Y, Sun W, Guo J, et al. In silico design of a DNA-based HIV-1 multiepitope vaccine for Chinese populations. Hum Vaccin Immunother. 2015;11(3):795–805. doi:10.1080/21645515.2015.1012017
[55] Ayyagari VS,Venkateswarulu TC, Karlapudi AP, et al. Design of a multiepitope-based vaccine targeting M-protein of SARS-CoV2: an immunoinformatics approach. J Biomol Struct Dyn. 2022 Apr;40(7):2963–2977. doi:10.1080/07391102.2020.1850357
[56] Livingston B, Crimi C, Newman M, et al. A rational strategy to design multiepitope immunogens based on multiple Th lymphocyte epitopes. J Immunol (Baltimore, Md: 1950). 2002 Jun 1;168(11):5499–5506. doi:10.4049/jimmunol.168.11.5499

[57] Sarkar B, Ullah MA, Johora FT, et al. Immunoinformatics-guided designing of epitope-based subunit vaccines against the SARS Coronavirus-2 (SARS-CoV-2). Immunobiology. 2020 May;225(3):151955. doi:10.1016/j.imbio.2020.151955

[58] Wiederstein M, Sippl MJ. ProSA-web: interactive web service for the recognition of errors in three-dimensional structures of proteins. Nucleic Acids Res. 2007 Jul;35(Web Server issue):W407–W410. doi:10.1093/nar/gkm290

[59] Kuna M, Mahdi F, Chade AR, et al. Molecular size modulates pharmacokinetics, biodistribution, and renal deposition of the drug delivery biopolymer elastin-like polypeptide. Sci Rep. 2018 May 21;8(1):7923. doi:10.1038/s41598-018-24897-9

[60] Huang X, Wang X, Zhang J, et al. Escherichia coli-derived virus-like particles in vaccine development. npj Vaccines. 2017/02/09;2(1):3. doi:10.1038/s41541-017-0006-8

[61] Mathur D, Prakash S, Anand P, et al. PEPlife: a repository of the falf-life of peptides. Sci Rep. 2016 Nov 07;6(1):36617. doi:10.1038/srep36617

[62] Naz A, Shahid F, Butt TT, et al. Designing multiepitope vaccines to combat emerging coronavirus disease 2019 (COVID-19) by employing immuno-informatics approach. Front Immunol. 2020;11:1663. doi:10.3389/fimmu.2020.01663

[63] Boyle MJ, Richards JS, Gilson PR, et al. Interactions with heparin-like molecules during erythrocyte invasion by Plasmodium falciparum merozoites. Blood. 2010 Jun 3;115(22):4559–4568. doi:10.1182/blood-2009-09-243725

[64] Spring MD, Pichyangkul S, Lon C, et al. Antibody profiles to plasmodium merozoite surface protein-1 in Cambodian adults during an active surveillance cohort with nested treatment study. Malar J. 2016 Jan 8;15:17. doi:10.1186/s12936-015-1058-8

[65] Yousaf H, Naz A, Zaman N, et al. Immunoinformatic and reverse vaccinology-based designing of potent multi-epitope vaccine against Marburgvirus targeting the glycoprotein. Heliyon. 2023 Aug;9(8):e18059. doi:10.1016/j.heliyon.2023.e18059

[66] Shah M, Rafiq S, Woo HG. Challenges and considerations in multi-epitope vaccine design surrounding toll-like receptors. Trends Pharmacol Sci. 2024 Dec;45(12):1104–1118. doi:10.1016/j.tips.2024.10.013

[67] Medzhitov R. Toll-like receptors and innate immunity. Nat Rev Immunol. 2001 Nov 1;1(2):135–145. doi:10.1038/35100529

[68] Perez-Mazliah D, Langhorne J. CD4 T-cell subsets in malaria: TH1/TH2 revisited. Front Immunol. 2014;5:671.